GEOPHYSICAL RESEARCH LETTERS, VOL. 20, NO. 6, PAGES 423-426, MARCH 19, 1993

THE ROLE OF DENSITY IN THE ACCUMULATION OF BASALTIC MELTS AT MID-OCEAN RIDGES

E.E. Hooft and R. S. Detrick

Department of Geology and Geophysics, Woods Hole Oceanographic Institution

Abstract. It is commonly assumed that magma ponds at a level of neutral buoyancy in the shallow crust where melt densities are equal to the bulk density of the surrounding crust. At the East Pacific Rise this neutral buoyancy level lies only 100-400 m below the sea floor, significantly shallower than the depths (> 1-2 km) of the magma bodies imaged in multichannel reflection data, suggesting that other factors must control the collection of melt in these reservoirs. The apparent inverse relationship between magma chamber depth and spreading rate at intermediate and fast spreading ridges suggests that the thermal structure of the rise axis, not the buoyancy of melt, is the primary factor that controls the depth at which melt ponds in crustal magma chambers beneath mid-ocean ridges.

Introduction

Multichannel seismic studies along the fast spreading East Pacific Rise (EPR) show the existence of a narrow (<1-4 km wide), thin (10s-100s of m thick) sill-like magma body 1-2 km below the sea floor (Detrick et al., 1987; Detrick et al., 1993). Despite its narrow width, reflections from the roof of this magma sill are remarkably continuous along the rise axis and relatively constant in two-way travel time below the sea floor over distances of many tens of kilometers. Along the northern EPR between 9°N and 13°N this reflector typically occurs $\geq$ 1.2-1.6 km below the sea floor (Detrick et al., 1987). Along the faster spreading southern EPR between the Garrett FZ and 20.7°S the magma sill is somewhat shallower with a median depth of 1.3 km, and in some locations (e.g. 14°14'S, 17°25'S) it rises to within 1000 m of the sea floor (Detrick et al., 1993). Similar axial reflectors have also been observed at intermediate-rate spreading ridges including the Juan de Fuca (Morton et al., 1987) and Valu Fa (Morton and Sleep, 1985; Collier and Sinha, 1990) ridges where they are significantly deeper (>3 km) than the magma bodies found along the EPR (Figure 1).

What controls the level of magma ponding beneath these spreading centers and the striking along-axis uniformity in the depth of magma sills apparent in multichannel seismic reflection data? It is commonly assumed that the ascent of magmas through the crust beneath magmatic systems is primarily driven by the buoyancy of the melt relative to the surrounding country rock (c.f. Ryan, 1987; Walker, 1989). When the density of the melt and that of the local crustal rocks are equal, the melt is neutrally buoyant and will tend to spread laterally instead of rising or sinking. The collection of melt at a level of neutral buoyancy (LNB) could explain the formation of the shallow, sill-like crustal magma bodies observed along mid-ocean ridges. However, factors other than density can affect the upward migration of melt within the crust. For example, the ascending melt may stall at a rheological boundary, like the brittle-ductile transition (Smith and Cann, 1992) or the freezing horizon (Phipps Morgan and Chen, 1993). The mechanics of dike formation and propagation and the state of stress in the shallow crust may also influence the accumulation of shallow magma reservoirs (Rubin, 1990; Gudmundsson, 1990).

In this paper we test the hypothesis that the magma bodies observed beneath mid-ocean ridges form at a LNB in the shallow crust by comparing the seismically constrained depths of ridge crest magma chambers with the depth of the LNB determined from estimates of melt and crustal density.

Estimation of melt and crustal densities

The LNB has been defined by Ryan (1987) as the depth in the crust where the magma density is equal to the local bulk density of the surrounding country rock. Below this level magma will be less dense than its surroundings and tend to rise, while above the LNB magma will be negatively buoyant and will sink. Therefore the LNB corresponds to the depth, z_{nb}, of the cross-over of the effective, large-scale *in situ* density of the crust, $\rho(z)$, with the magma density, ρ_m. To estimate the LNB at the EPR we must know both the magma density, ρ_m, and the variation of density with depth in oceanic crust, $\rho(z)$.

Melt Density: The density of the liquid from which a basaltic glass formed can be computed using the empirical method of Bottinga and Weill (1970). They determined the

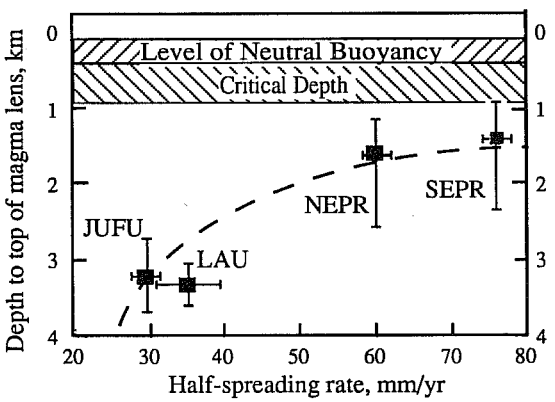

Fig 1. Depth to the top of the AMC versus spreading rate for the northern (NEPR) and southern (SEPR) East Pacific Rise, and Juan de Fuca (JUFU) and Valu Fau (LAU) ridges (replotted from Phipps Morgan and Chen, 1993). The neutral buoyancy level and critical depth calculated for the EPR are also shown. The dashed curve represents the predicted depth to the solidus (assumed to be 1200°C) as a function of spreading rate from Phipps Morgan and Chen (1993).

Paper number 93GL00295
0094-8534/93/93GL-00295$03.00

partial molar volume of the major oxide components in a liquid and thence the density of a silicate melt as a function of major oxide composition and temperature.

Using these equations melt densities were calculated for the entire Smithsonian Institution Glass file consisting of 2004 samples of basaltic glasses from around the world's oceans. A plot of melt density versus Fe# (Fe/(Fe+Mg), shown in Figure 2, follows the theoretical curves predicted for the evolution of residual basaltic liquids (Stolper and Walker, 1980). Most oceanic basalts lie in the density minimum of this evolution curve suggesting that melt density is an important factor in determining the eruptability of magmas (Stolper and Walker, 1980). The average melt density is 2700 kgm^{-3}; 73% of the samples lie within a range of ± 20 kgm^{-3} from this value.

We will adopt a value of 2700 ± 20 kgm^{-3} for ρ_m in this paper. Density increases due to continued crystal fractionation (for the range of eruptable basalts) are only a few percent of this average melt density and will not significantly effect our results. Volatiles can lower melt densities, especially if exsolution of these gases occurs. But, the volatile content of MORB is in general very low and the effect of volatiles on density will be small while remaining dissolved (e.g. 0.25% H_2O will reduce the melt densities by only 20 kgm^{-3}). Thus the effects of fractional crystallization and volatiles on melt density are second order and largely offsetting.

Crustal Density Structure: Seismic studies at the EPR (e.g. Vera et al., 1990; Christeson et al., 1992) document the presence of a near-surface layer, ~150 m thick at the rise axis, of extremely low (< 3 km/s) compressional wave velocities (Figure 3a). Below this layer p-wave velocities increase rapidly to ~5 km/s at 300 m and ~6 km/s 1-1.2 km below the sea floor. The low seismic velocities observed in the upper kilometer of the crust are due to high bulk porosities caused by the presence of fractures and voids too large to be sampled in the laboratory. An accurate estimate of the crustal density structure at a ridge crest thus requires a knowledge of the variation in bulk porosity with depth in oceanic crust.

The only *in situ* measurements of bulk porosity to substantial depths within young oceanic crust have been made in Hole 504B on ~5.9 Ma old sea floor on the flanks of the Costa Rica Rift in the eastern equatorial Pacific. Large-scale electrical resistivities measured in this borehole (e.g. Becker, 1985) have been used to calculate apparent bulk porosities using Archie's law (Figure 3b). Bulk porosities are high (10-

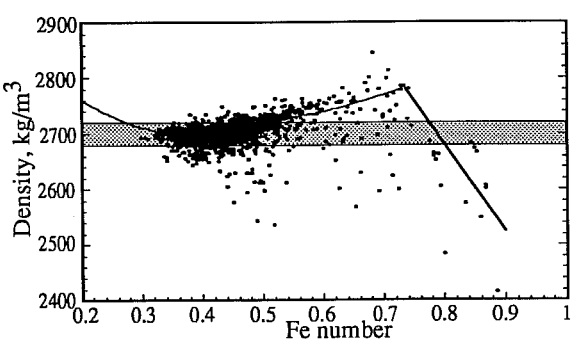

Fig 2. Plot of melt density for MOR basaltic glasses versus the degree of fractionation represented by the Fe#= Fe/(Fe+Mg). The curve shows the evolution of residual melt during fractional crystallization (Stolper and Walker, 1980). The mean melt density is 2700 ± 20 kgm^{-3} (shaded bar).

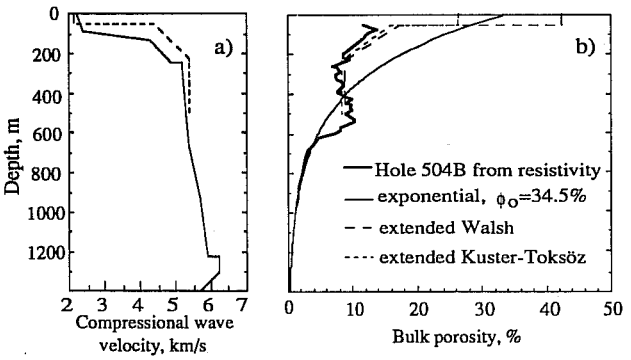

Fig 3. (Left) Seismic velocity models of the EPR crest near 9°30'N after Christeson et al. (1992) (dashed line) and Vera et al. (1990) (solid line). (Right) Variation of crustal bulk porosity with depth in young oceanic crust: based on *in situ* measurements in Hole 504B (from Becker et al., 1985), theoretical velocity-porosity relationships based on extended Walsh and Kuster-Toksöz theories (from Berge et al., 1992), and an exponential decrease in bulk porosity with depth (ϕ_o =34.5%; $\lambda = 3.3*10^{-3}$ m^{-1}).

15%) in the shallowmost crust, decrease to 7-10% within the lower part of the extrusive section (200-600 m sub-basement) then drop sharply to values of <1-2% in the underlying sheeted dike section. Bulk porosities remain extremely low (<1%) throughout the sheeted dike section to the base of present hole (1726 m sub-basement).

In situ measurements of crustal physical properties have not been made at the EPR. However, an estimate of crustal porosity and bulk density can be obtained by using observed seismic velocities at the rise axis and theoretical predictions of the variation in seismic velocity as a function of pore volume and aspect ratio. Classical Hashin-Shtrikman limits on the relationship between porosity and seismic velocity ignore void shapes and are too broad to provide useful constraints. However, Berge et al. (1992) have devised two hybrid theories, which they call the extended Walsh and extended Kuster-Toksöz theories which provide upper and lower bounds on effective medium properties for porosities of up to 30% and a distribution of pore aspect ratios representative of the upper oceanic crust (Wilkens et al., 1991). Figure 3b shows the variation in porosity with depth predicted using these theories for the Christeson et al. (1992) seismic model of the EPR shown in Figure 3a. Bulk crustal porosities are very high (26-43%) in the upper 100 m then decrease to values of less than 10% 200 m into the crust. Note that below 100 m into basement the results are in close agreement with *in situ* bulk porosity measurements made at Hole 504B. Below about 700 m depth large-scale crustal porosity decreases exponentially with depth (Figure 3b).

Porosity and density are inversely related and the bulk density at any depth z below the sea floor can be directly calculated from the bulk porosity, $\phi(z)$, using the expression:

$$\rho(z) = \rho_g - \phi(z)\,(\rho_g - \rho_w) \qquad (1)$$

where $\rho_g = 2950$ kgm^{-3} is the matrix grain density and the density of water, $\rho_w = 1000$ kgm^{-3}. Figure 4a shows $\rho(z)$ for the two EPR crustal porosity models of Berge et al. (1992). Also shown is $\rho(z)$ calculated assuming an exponential decrease in porosity with depth:

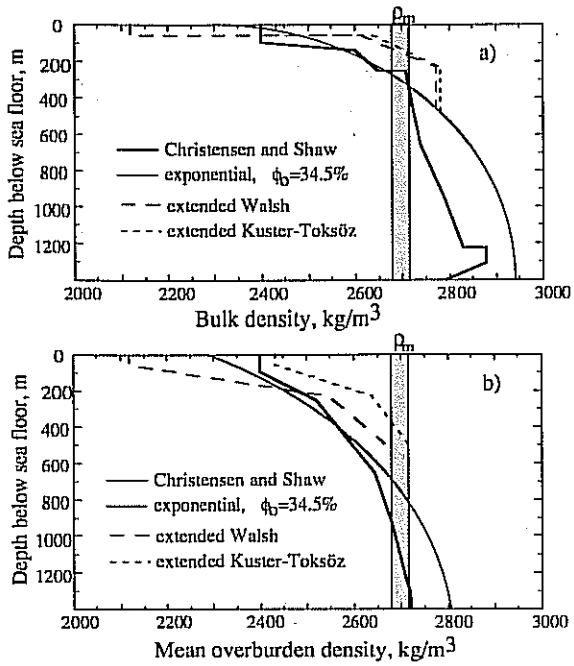

Fig 4. (Top) Crustal density versus depth in young oceanic crust based on the bulk porosity estimates shown in Fig. 3. Also shown is a density model based on the EPR seismic velocity model of Vera et al (1990) calculated using the empirical velocity-density equation of Christensen and Shaw (1970): $\rho = 1.85 + 0.165\ V_p$. The shaded bar represents the mean magma density from Fig. 2. The LNB at the EPR is lies at 100-400 m depth. (Bottom) Variation in mean overburden density versus depth. These curves were calculated from the four density models shown above. The critical depth, z_c, at the EPR is located at 400-900 m depth.

$$\phi(z) = \phi_0\, e^{-\lambda z} \qquad (2)$$

with an assumed surface porosity, ϕ_0, of 34.5% and λ=3.3*10^{-3} m^{-1}. This function is consistent with the high near-surface crustal porosities inferred seismically at the EPR and provides a good fit to the decrease in *in situ* porosities measured in Hole 504B below 600 m depth (Figure 3b).

An independent estimate of the density structure of oceanic crust at the EPR can be obtained by converting measured seismic crustal velocities to density using empirical relationships determined from laboratory measurements of compressional wave velocity and density made on oceanic dredge samples (Christensen and Shaw, 1970). Because laboratory velocity measurements don't take into account large-scale crustal porosity, this approach will be most accurate for the deeper parts of the crustal section. The seismic structure of the rise axis was taken from an expanding spread profile shot along the crest of the EPR at 9°N (Vera et al., 1990). The resulting $\rho(z)$ curve is plotted in Figure 4a. Note that the decrease in compressional wave velocity between 1.2 and 1.6 km depth in the Vera et al. (1990) model marks the top of the axial magma chamber; the inferred decrease in crustal density below this depth is due to the presence of magma and is not an intrinsic feature of the density structure of oceanic crust.

The three different methods of estimating the density structure of oceanic crust at the EPR described above all provide remarkably consistent results (Figure 4a). Bulk crustal densities are expected to be very low (<2500 kgm^{-3}) in the upper 100 m of the crust. They increase rapidly to about 2700 kgm^{-3} ~150-400 m into the crust, and reach values of 2800-2900 kgm^{-3} at 1000 m depth.

Discussion

A LNB will exist in the shallow oceanic crust where the average melt density (2700 $\pm$ 20 kgm^{-3}) intersects the crustal density curve. For the data shown in Figure 4a the LNB is located about 100-400 m below the sea floor at the EPR. The LNB cannot lie significantly deeper than this at the EPR without being in serious disagreement with the known seismic velocity structure of the EPR, theoretical and empirical relationships between seismic velocity, bulk porosity and density, and *in situ* measurements of the physical properties of young oceanic crust.

If density were the principal factor controlling the accumulation of melt beneath mid-ocean ridges, as some investigators have suggested (e.g. Ryan, 1987), we would expect crustal magma bodies to form at the depth of this LNB, i.e. about 100-400 m below the sea floor. However, the axial magma chambers documented seismically along the EPR occur 1-2 km below the sea floor, well below the calculated depth of the LNB (Figure 1). Even along the fast spreading southern EPR, where the shallowest crustal magma bodies have been documented, the top of the magma sill is typically more than 1000 m below the sea floor (Detrick et al., 1993). Along the Juan de Fuca (Morton et al., 1987) and Valu Fa (Morton and Sleep, 1985; Collier and Sinha, 1990) ridges magma chambers lie deeper than 3 km. We thus conclude that magma chambers beneath intermediate and fast spreading ridges do not form at a LNB and other factors must control the accumulation of melt beneath mid-ocean ridges.

All of the mid-ocean ridge magma chambers observed to date lie at or below what we call the critical depth, z_c, the depth below which lithostatic pressure alone provides enough hydrostatic head to force magma from the reservoir to the surface. At the critical depth $\rho_{av}(z_c) = \rho_m$ where $\rho_{av}(z)$ is the mean overburden density at depth z.

Figure 4b shows the mean overburden density versus depth, $\rho_{av}(z)$, calculated for the four crustal density models shown in Figure 4a. Our best estimate of the critical depth at the EPR is that it lies 400-900 m below the sea floor. The axial magma chambers imaged seismically at the EPR occur close to, but below, the critical depth while those found along the intermediate spreading Valu Fa and Juan de Fuca Ridges lie well below the critical depth (Figure 2). Magma that ponds above the critical depth may still be eruptable since other mechanisms may increase magma reservoir pressures above this minimum value, but for magma bodies lying below the critical depth lithostatic pressure alone is sufficient to insure eruptability provided a continuous pressure connection (e.g. a dike) exists with the surface.

If magma ponds at mid-ocean ridges in crustal reservoirs well below the LNB, as the evidence presented in this paper strongly suggests, what stops the buoyancy-driven ascent of melt through the crust? The answer to this question is not entirely clear. Gudmundsson (1990) has proposed that rapid injections of dikes at a fast spreading ridge create a stress barrier in the mid-crust where the horizontal compressive stress is higher than the vertical stress causing sill formation

that leads to the development of a mid-crustal magma chamber. Rubin (1990) showed that in regions undergoing active extension, the brittle-ductile boundary may become a depth of "effective" neutral buoyancy due to the accumulation of non-hydrostatic, tectonically-induced stress differences. Phipps Morgan and Chen (1993) have proposed that melt will be stopped in its upward ascent when it reaches the freezing horizon due to viscous stresses that favor magma ponding.

Whether it is the brittle-ductile boundary or the freezing horizon that effectively stops the upward ascent of melt, the depth of both will be primarily controlled by the thermal structure of the crust at the ridge axis. The strongest evidence for a thermal control on the depth at which magma accumulates beneath mid-ocean ridges is the variation in depth of crustal magma chambers with spreading rate, first noted by Purdy et al. (1992), and illustrated in Figure 1. The hypothesis that the depth of magma bodies beneath mid-ocean ridges are primarily controlled by thermal processes has recently been tested quantitatively by Phipps Morgan and Chen (1993). They show that the depth of the 1200°C isotherm varies with spreading rate in a way that is consistent with the variation in the depth to axial magma bodies determined seismically along intermediate and fast spreading ridges (Figure 1). Their results, and the seismic evidence that axial magma chambers lie below the LNB, support the hypothesis that the buoyancy of melt is not the primary factor controlling the depth of magma bodies beneath ridge crests.

Conclusions

1. The crustal magma bodies observed beneath mid-ocean ridges do not form at a level of neutral buoyancy in the shallow crust. The neutral buoyancy level lies only 100-400m below the sea floor, much shallower than the depth (1-3 km) of the axial magma bodies imaged in multichannel reflection data at intermediate and fast spreading ridges.

2. The magma bodies found along mid-ocean ridges are located at or below the critical depth where lithostatic pressure due to the integrated weight of the overlying crustal column alone is sufficient for magma to be erupted onto the sea floor.

3. The apparent inverse relationship between magma chamber depth and spreading rate at intermediate and fast spreading ridges suggests that the thermal structure of the rise axis is the primary factor that controls the depth at which melt ponds in crustal magma chambers beneath mid-ocean ridges.

Acknowledgments. This research was supported by NSF grant OCE-9296017. E. Hooft was supported by the WHOI Joint Program Education Office. W. Bryan stimulated the calculation of melt densities. Joe Cann, Jian Lin and Deborah Smith provided helpful discussions, as did two anonymous reviewers. WHOI contribution 8176.

References

Becker, K., Large scale electrical resistivity and bulk porosity of the oceanic crust, DSDP Hole 504B, Costa Rica Rift, Init. Rep. Deep Sea Drill. Proj., 83, 419-427, 1985.

Berge, P., G. Fryer, G. and R. Wilkens, Velocity-porosity relationships in the upper oceanic crust: Theoretical considerations, J. Geophys. Res., 97, 15,239-15,254, 1992.

Bottinga, Y. and D.F. Weill, Densities of liquid silicate systems calculated from partial molar volumes of oxide components, Amer. J. Sci., 269, 169-182, 1970.

Christensen, N.I., and G.H. Shaw, Elasticity of mafic rocks from the mid-Atlantic ridge, Geophys. J. Roy. Astron. Soc., 20, 271-284, 1970.

Christeson, G.L., G.M. Purdy and G.J. Fryer, Structure of young upper crust at the East Pacific Rise near 9°30'N, Geophys. Res. Lett., 19, 1045-1048, 1992.

Collier, J. and M. Sinha, Seismic images of a magma chamber beneath the Lau Basin back-arc spreading center, Nature, 346, 646-648, 1990.

Detrick, R.S., P. Buhl, E. Vera, J. Mutter, J. Orcutt, J. Madsen, and T. Brocher, Multi-channel seismic imaging of a crustal magma chamber along the East Pacific Rise, Nature, 326, 35-41, 1987.

Detrick, R.S., A.J. Harding, G.M. Kent, J.A. Orcutt, J.C. Mutter, P. Buhl , Seismic structure of the southern East Pacific Rise, Science, 259, 499-503, 1993.

Gudmundsson, A., Emplacement of dikes, sills and crustal magma chambers at divergent plate boundaries, Tectonophys., 176, 257-275, 1990.

Morton, J.L., and N.H. Sleep, Seismic reflections from the Lau Basin magma chamber. In: Geology and offshore resources of Pacific island arcs - Tonga region, Circum Pacific Council of Energy and Mineral Resources Earth Sciences Series, eds. D.W. Scholl and T.L. Vallier, pp.441-453, 1985.

Morton, J.L., N.H. Sleep, W.R. Normark and D.H. Tomkins, Structure of the southern Juan de Fuca Ridge from seismic reflection records, J. Geophys. Res., 92, 11,315-11,326, 1987.

Phipps Morgan, J., and Y.J. Chen, The genesis of oceanic crust: Magma injection, hydrothermal circulation, and crustal flow, J. Geophys. Res., in press

Purdy, G.M. L. Kong, G. Christeson and S. Solomon, Relationship between spreading rate and the seismic structure of mid-ocean ridges, Nature, 355, 815-817, 1992.

Ryan, M.P., Neutral buoyancy and the mechanical evolution of magmatic systems, Geochem. Soc. Spec. Pub. No. 1, 1987.

Rubin, A.M., A comparison of rift-zone tectonics in Iceland and Hawaii, Bull. Volcanol., 52, 302-319, 1990.

Smith, D.K. and J.R. Cann, The role of seamount volcanism in crustal construction at the mid-Atlantic ridge (24°N-30°N), J. Geophys. Res., 97, 1645-1658, 1992.

Stolper, E.and D. Walker, Melt density and the average composition of basalt, Contrib. Mineral. Pterol., 74, 7-12, 1980.

Vera, E.E., J. Mutter, P. Buhl, J. Orcutt, A. Harding, M. Kappus, R. Detrick, and T. Brocher, The structure of 0- to 0.2-m.y.-old oceanic crust at 9°N on the East Pacific Rise from expanded spread profiles, J. Geophys. Res., 95, 15,529-15,556, 1990.

Walker, G.P.L., Gravitational (density) controls on volcanism, magma chambers and intrusions, Australian J. Earth Sci., 36, 149-165, 1989.

Wilkens, R.H., G.J. Fryer, J. Karsten, Evolution of porosity and seismic structure of the upper oceanic crust: Importance of aspect ratios, J. Geophys. Res., 96, 17,981-17,995, 1991.

E.E. Hooft and R.S. Detrick, Department of Geology and Geophysics, Woods Hole Oceanographic Institution, Woods Hole, MA 02543.

(Received September 25, 1992;
revised January 12, 1993;
accepted Febuary 1, 1993.)